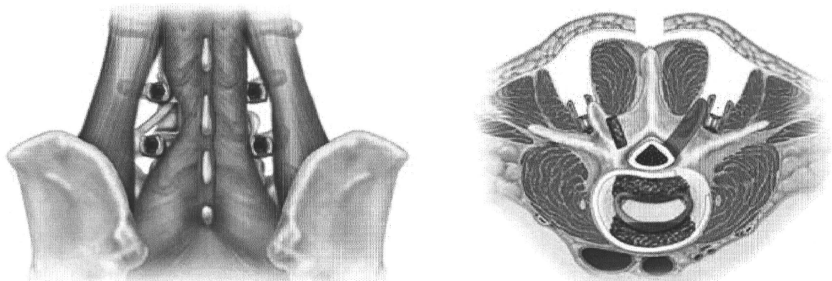


## Paraspinal TLIF for lumbar foraminal stenosis



**FIG. 3.** Artist's illustration of the paraspinal-approach TLIF. **Left:** Bilateral paraspinal approach, placement of the PS, and exposure of the neural foramen after excision of the unilateral facet joint. **Right:** Interbody placement of the titanium cage combined with porous hydroxyapatite spacer and grafting of autologous local bone chips around the cage and contralateral facet joint.

stability. An MR imaging study showed bilateral foraminal stenosis combined with a right-side lateral herniated disc at the L5–S1 level (Fig. 4A and B). A preoperative L-5 nerve root injection effectively controlled his leg pain for a few days. The operative procedure was paraspinal TLIF at L5–S1 (Fig. 4C and D). Pedicle screw placement in the inversion angle was achieved through a paraspinal approach. The operating time was 150 minutes, and the estimated intraoperative blood loss was 230 ml. At 6 months after the operation, CT showed successful bony union (Fig. 4E), MR imaging showed a Grade 1 change

of the paravertebral muscle on both sides (Fig. 4F), and the patient was free of complaints with a full JOA score of 29 points.

### Discussion

Sixteen patients with lumbar foraminal stenosis were treated successfully using a paraspinal-approach TLIF. Marked improvements in clinical outcomes and low incidence of paraspinal muscle injury represent the potential benefits of minimally invasive spinal fusion technique.

**TABLE 3: Summary of clinical and radiological outcomes\***

Case No.	Op Time (min)	Blood Loss (ml)	Bone Graft	Postop JOA	Recovery Rate (%)	Bony Union	MRI Grading† (rt/lt)	Complication	ASD	FU Period (mos)
1	168	139	local	29	100	union	0/0	none	HNP	45
2	203	144	local	29	100	union	1/1	none	none	43
3	196	465	local	27	86.6	union	1/0	none	none	30
4‡	136	300	iliac	—	—	union	1/1	none	none	27
5	211	227	local	24	58.3	union	—	none	none	27
6	150	230	local	29	100	union	0/1	none	none	25
7	192	205	HA + local	29	100	union	1/1	PS misplacement	none	24
8	200	440	HA + local	29	100	union	1/1	none	none	23
9	289	720	local	23	60	union	—	none	none	19
10	206	206	HA + local	29	100	union	L3–4 1/1, L4–5 1/1	none	none	18
11	147	120	iliac	23	70	union	1/1	none	none	17
12	230	328	iliac	29	100	union	L3–4 1/0, L4–5 2/2	none	none	16
13	185	200	HA + local	29	100	union	1/1	none	none	16
14	140	30	iliac	28	91.6	union	0/1	none	none	15
15	218	530	iliac	26	85.7	union	L3–4 1/1, L4–5 2/2	none	none	12
16	130	100	HA + local	28	85.7	union	0/0	none	none	12

\* ASD = adjacent-segment disease; FU = follow-up; HA = hydroxyapatite spacer; HNP = herniated nucleus pulposus.

† Grades on MR imaging defined as follows: Grade 0, no signal change; Grade 1, signal change in less than 50% of area; Grade 2, signal change in more than 50% of area; Grade 3, signal change in more than 50% of area with atrophy.

‡ This patient had rheumatoid arthritis and was excluded from the JOA score and recovery rate assessment.

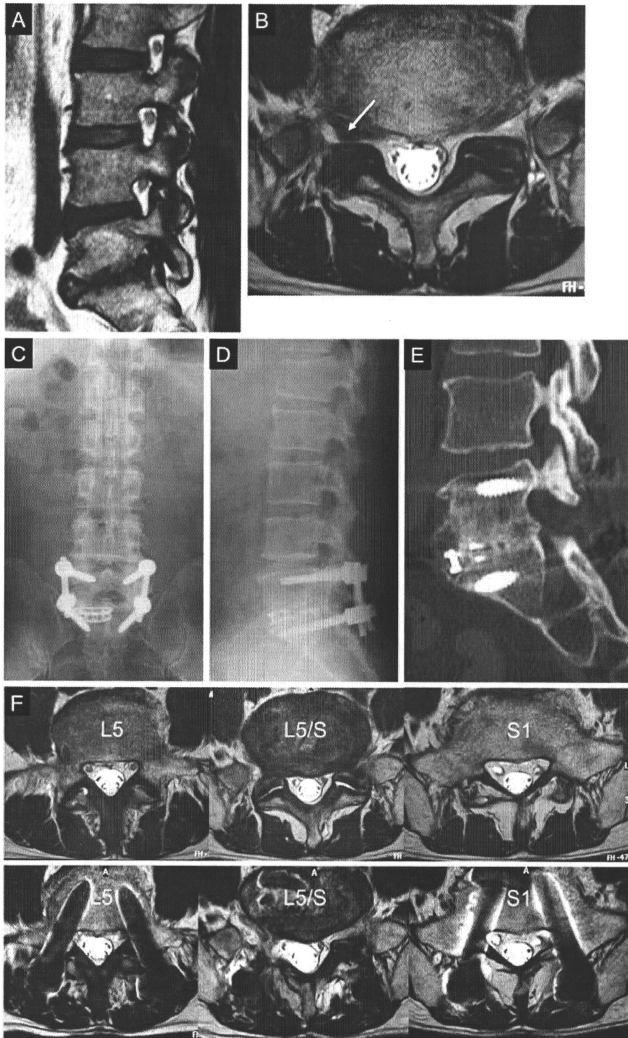


Fig. 4. Case 6. Preoperative and postoperative radiological studies obtained in a 58-year-old man with foraminal stenosis combined with lateral disc herniation at L5–S1. **A**: Parasagittal MR image demonstrating foraminal stenosis with a Modic change of the vertebral endplate. **B**: Axial MR image demonstrating foraminal stenosis with lateral disc herniation (*arrow*) on the right side at the L5–S1 level. **C and D**: Anteroposterior and lateral radiographs demonstrating good positioning of the interbody cage and PSs. **E**: Sagittal reconstruction CT image demonstrating solid bony union into and around the cage 6 months after surgery. **F**: Axial MR images demonstrating minimal changes in the paraspinal muscles before surgery (*upper*) and 6 months after surgery (*lower*).

## Paraspinal TLIF for lumbar foraminal stenosis

Unrecognized or recurrent foraminal stenosis may be associated with failed back surgery syndrome. In a review of failed back surgery syndrome, Burton et al.<sup>4</sup> attributed the condition to the lack of recognition or inadequate treatment of nonspecific lateral canal stenosis and considered it to be the cause of pain in nearly 60% of patients with continued postoperative symptoms. Adequate preoperative diagnosis of foraminal lesions is important to achieving successful surgical results. Parasagittal and coronal MR images and axial and parasagittal CT images are mainstays for evaluating and quantifying the degree of foraminal stenosis. However, the false-positive and false-negative rates are high.<sup>1,2</sup> Concordance of imaging studies, selective nerve root block, and clinical symptoms are the keys to making a correct diagnosis. In the current study, all but 1 patient, who was paralytic, experienced immediate pain relief after selective nerve root block, which reflected the correct diagnosis and subsequent successful surgical results.

The disadvantages of decompressive surgery via interlaminar or/and extralaminar access include incomplete decompression and blind maneuvers around the DRG. Because the transformal ligaments are attached to the superior articular facet, the superior articular facet must be excised to expose the neural foramen completely.<sup>16</sup> The DRG is sensitive to mechanical pressure, and excessive manipulation of the DRG leads to worsening postoperative symptoms, such as persistent dysesthesia and complex regional pain syndrome Type I.<sup>19</sup> In addition, excessive facet and annulus removal at the time of decompression increases the possibility of postoperative segmental instability and asymmetrical disc space collapse and leads to poor surgical results.<sup>5</sup>

The insertion of an interbody implant allows the distraction of the disc space and subsequent enlargement of the intervertebral foramen. Posterior lumbar interbody fusion is considered an indirect foraminal enlargement procedure. In this procedure, the posterior midline structures such as the paravertebral muscle, spinous process, and laminae must be excised to place the intervertebral implants, and this procedure may cause postoperative denervation of posterior structures.<sup>9,15,23,28</sup> In addition, medial retraction of the traversing nerve root and dural tube is necessary to place the intervertebral implants, and this may cause neural tissue damage and epidural scar formation.

A paraspinal-approach TLIF is a safe and minimally invasive procedure that can be used to decompress and stabilize lesions in the stenotic foramen. The paraspinal approach to the lumbar spine was introduced by Wiltse.<sup>26,29,30</sup> The lateral parts of the facet joint can be exposed easily by blunt dissection through the cleavage plane between the multifidus and the longissimus parts of the sacrospinalis muscle at the cranial to L4–5 level. In cases involving L5–S1 exposure, detachment of the multifidus muscle from the longissimus parts of the sacrospinalis allows good visualization because the multifidus muscle courses obliquely and dorsolaterally to attach to the longissimus parts of the sacrospinalis and the ilium.<sup>27</sup> The paraspinal approach can allow good visualization and maintain a wide field for the surgical maneuver. Di-

rect visualization of compressive pathologies by complete removal of the facet joint and surrounding soft tissue, and stabilization of unstable spinal segments to resolve the dynamic lesion at the same time, are safe and secure procedures. The TLIF has the following advantages: 1) It requires a single midline skin incision. 2) It is minimally invasive to the posterior midline structure. 3) It allows medially oriented PS placement. 4) It allows direct visualization and decompression of the intraforaminal lesion. 5) It requires an easily applied distraction and compression maneuver through manipulation of the collapsed disc space and the placed PSs. 6) Disc space enlargement can be achieved by the placement of an interbody spacer. 7) It permits a combination of contralateral facet fusion to achieve circumferential fusion.

Postoperative MR imaging confirmed the minimal invasiveness on the posterior structures. In the current series, in patients with a single-level fusion, the muscle injury grade was limited to 0–1. In contrast, 2 of the patients with a double-level fusion exhibited Grade 2 injury at the caudal level, although the radiological results were not related to the clinical results. A possible disadvantage of the paraspinal approach is direct injury to the medial, muscular, or lateral branch of the posterior ramus, which is related to denervation of the multifidus muscle. The surgeon should be aware that multilevel fusion through the paraspinal approach has potential to cause direct nerve injury and subsequent muscle denervation.

## Conclusions

Sixteen patients with lumbar foraminal stenosis were treated successfully using a paraspinal-approach TLIF. We conclude that the paraspinal-approach TLIF is a minimally invasive, safe, and secure procedure to treat lumbar foraminal lesions. Direct visualization and decompression of the foraminal lesion, distraction of the disc space by the placement of an interbody spacer, and stabilization of unstable segments can be achieved simultaneously through the paraspinal approach, which produces successful clinical and radiological outcomes.

## Disclosure

The authors report that no funds were received in support of this study and no benefits in any form have been or will be received from a commercial party related directly or indirectly to the subject of this manuscript.

Author contributions to the study and manuscript preparation include the following. Conception and design: Fujibayashi. Acquisition of data: Fujibayashi. Analysis and interpretation of data: Fujibayashi. Drafting the article: Fujibayashi. Critically revising the article: Fujibayashi. Reviewed final version of the manuscript and approved it for submission: all authors. Statistical analysis: Fujibayashi. Study supervision: Neo, Nakamura.

## References

1. Aota Y, Niwa T, Yoshikawa K, Fujiwara A, Asada T, Saito T: Magnetic resonance imaging and magnetic resonance myelography in the presurgical diagnosis of lumbar foraminal stenosis. *Spine* 32:896–903, 2007
2. Attias N, Hayman A, Hipp JA, Noble P, Esses SI: Assessment

- of magnetic resonance imaging in the diagnosis of lumbar spine foraminal stenosis—a surgeon's perspective. **J Spinal Disord Tech** 19:249–256, 2006
3. Blume HG: Unilateral posterior lumbar interbody fusion: simplified dowel technique. **Clin Orthop Relat Res** 193:75–84, 1985
  4. Burton CV, Kirkaldy-Willis WH, Yong-Hing K, Heithoff KB: Causes of failure of surgery on the lumbar spine. **Clin Orthop Relat Res** 157:191–199, 1981
  5. Chang SB, Lee SH, Ahn Y, Kim JM: Risk factor for unsatisfactory outcome after lumbar foraminal and far lateral microdecompression. **Spine** 31:1163–1167, 2006
  6. Cinotti G, De Santis P, Nofroni I, Postacchini F: Stenosis of lumbar intervertebral foramen: anatomic study on predisposing factors. **Spine** 27:223–229, 2002
  7. Dhall SS, Wang MY, Mummaneni PV: Clinical and radiographic comparison of mini-open transforaminal lumbar interbody fusion with open transforaminal lumbar interbody fusion in 42 patients with long-term follow-up. **J Neurosurg Spine** 9:560–565, 2008
  8. Fujiwara A, An HS, Lim TH, Haighton VM: Morphologic changes in the lumbar intervertebral foramen due to flexion-extension, lateral bending, and axial rotation: an in vitro anatomic and biomechanical study. **Spine** 26:876–882, 2001
  9. Gejo R, Matsui H, Kawaguchi Y, Ishihara H, Tsuji H: Serial changes in trunk muscle performance after posterior lumbar surgery. **Spine** 24:1023–1028, 1999
  10. Harms JG, Jeszensky D: The unilateral transforaminal approach for posterior lumbar interbody fusion. **Orthop Traumatol** 6:88–99, 1998
  11. Inufusa A, An HS, Lim TH, Hasegawa T, Haighton VM, Nowicki BH: Anatomic changes of the spinal canal and intervertebral foramen associated with flexion-extension movement. **Spine** 21:2412–2420, 1996
  12. Jenis LG, An HS: Spine update. Lumbar foraminal stenosis. **Spine** 25:389–394, 2000
  13. Kunogi J, Hasue M: Diagnosis and operative treatment of intraforaminal and extraforaminal nerve root compression. **Spine** 16:1312–1320, 1991
  14. Lee DY, Jung TG, Lee SH: Single-level instrumented mini-open transforaminal lumbar interbody fusion in elderly patients. **J Neurosurg Spine** 9:137–144, 2008
  15. Macnab I, Cuthbert H, Godfrey CM: The incidence of denervation of the sacrospinales muscles following spinal surgery. **Spine** 2:294–298, 1977
  16. Min JH, Kang SH, Lee JB, Cho TH, Suh JG: Anatomic analysis of the transforaminal ligament in the lumbar intervertebral foramen. **Neurosurgery** 57 (1 Suppl):37–41, 2005
  17. Mummaneni PV, Rodts GE Jr: The mini-open transforaminal lumbar interbody fusion. **Neurosurgery** 57 (4 Suppl):256–261, 2005
  18. Potter BK, Freedman BA, Verwiebe EG, Hall JM, Polly DW Jr, Kuklo TR: Transforaminal lumbar interbody fusion: clinical and radiographic results and complications in 100 consecutive patients. **J Spinal Disord Tech** 18:337–346, 2005
  19. Raja SN, Grabow TS: Complex regional pain syndrome I (reflex sympathetic dystrophy). **Anesthesiology** 96:1254–1260, 2002
  20. Scheufler KM, Dohmen H, Vougioukas VI: Percutaneous transforaminal lumbar interbody fusion for the treatment of degenerative lumbar instability. **Neurosurgery** 60 (4 Suppl 2):203–213, 2007
  21. Schneiderman G, Flannigan B, Kingston S, Thomas J, Dillin WH, Watkins RG: Magnetic resonance imaging in the diagnosis of disc degeneration: correlation with discography. **Spine** 12:276–281, 1987
  22. Schwender JD, Holly LI, Rouben DP, Foley KT: Minimally invasive transforaminal lumbar interbody fusion (TLIF): technical feasibility and initial results. **J Spinal Disord Tech** 18 (Suppl):S1–S6, 2005
  23. Sihvonen T, Herno A, Paljärvi L, Airaksinen O, Partanen J, Tapaninaho A: Local denervation atrophy of paraspinal muscles in postoperative failed back syndrome. **Spine** 18:575–581, 1993
  24. Taneichi H, Suda K, Kajino T, Matsumura A, Moridaira H, Kaneda K: Unilateral transforaminal lumbar interbody fusion and bilateral anterior-column fixation with two Brantigan I/F cages per level: clinical outcomes during a minimum 2-year follow-up period. **J Neurosurg Spine** 4:198–205, 2006
  25. Vanderlinden RG: Subarticular entrapment of the dorsal root ganglion as a cause of sciatic pain. **Spine** 9:19–22, 1984
  26. Vialle R, Wicart P, Drain O, Dubouset J, Court C: The Wiltse parasagittal approach to the lumbar spine revisited: an anatomic study. **Clin Orthop Relat Res** 445:175–180, 2006
  27. Weaver EN Jr: Lateral intramuscular planar approach to the lumbar spine and sacrum. Technical note. **J Neurosurg Spine** 7:270–273, 2007
  28. Weber BR, Grob D, Dvorák J, Müntener M: Posterior surgical approach to the lumbar spine and its effect on the multifidus muscle. **Spine** 22:1765–1772, 1997
  29. Wiltse LL: The parasagittal sacrospinalis-splitting approach to the lumbar spine. **Clin Orthop Relat Res** 91:48–57, 1973
  30. Wiltse LL, Bateman JG, Hutchinson RH, Nelson WE: The parasagittal sacrospinalis-splitting approach to the lumbar spine. **J Bone Joint Surg Am** 50:919–926, 1968

Manuscript submitted August 24, 2009.

Accepted April 6, 2010.

Address correspondence to: Shunsuke Fujibayashi, M.D., Ph.D., Department of Orthopaedic Surgery, Graduate School of Medicine, Kyoto University, 54 Shogoin Kawahara-cho, Sakyo-ku, Kyoto 606-8507, Japan. email: shfuji@kuhp.kyoto-u.ac.jp.

# Computer-Assisted Spinal Osteotomy

## A Technical Note and Report of Four Cases

Shunsuke Fujibayashi, MD, PhD,\* Masashi Neo, MD, PhD,\* Mitsuru Takemoto, MD, PhD,\*  
Masato Ota, MD,\* Tomitaka Nakayama, MD, PhD,\* Junya Toguchida, MD, PhD,†  
and Takashi Nakamura, MD, PhD\*

**Study Design.** A report of 4 cases of spinal osteotomy performed under the guidance of a computer-assisted navigation system and a technical note about the use of the navigation system for spinal osteotomy.

**Objective.** To document the surgical technique and usefulness of computer-assisted surgery for spinal osteotomy.

**Summary of Background Data.** A computer-assisted navigation system provides accurate 3-dimensional (3D) real-time surgical information during the operation. Although there are many reports on the accuracy and usefulness of a navigation system for pedicle screw placement, there are few reports on the application for spinal osteotomy.

**Methods.** We report on 4 complex cases including 3 solitary malignant spinal tumors and 1 spinal kyphotic deformity of ankylosing spondylitis, which were treated surgically using a computer-assisted navigation system. The surgical technique and postoperative clinical and radiologic results are presented.

**Results.** 3D spinal osteotomy under the guidance of a computer-assisted navigation system was performed successfully in 4 patients. All malignant tumors were resected *en bloc*, and the spinal deformity was corrected precisely according to the preoperative plan. Pathologic analysis confirmed the *en bloc* resection without tumor exposure in the 3 patients with a spinal tumor.

**Conclusion.** The use of a computer-assisted navigation system will help ensure the safety and efficacy of a complex 3D spinal osteotomy.

**Key words:** computer-assisted navigation system, spinal osteotomy, spinal tumor, ankylosing spondylitis. **Spine** 2010;35:E895–E903

Computer-assisted surgery was developed to decrease the intraoperative radiologic exposure to patients and physicians, to increase the accuracy of surgery, and to allow the surgeon to perform spine surgery safely. Many recent reports show that a computer-assisted navigation system increases the accuracy of pedicle screw place-

ment.<sup>1,2</sup> The usefulness of such navigation systems in the excision of ossification of the posterior longitudinal ligament, ossification of the ligamentum flavum, and some kinds of spinal tumors have also been reported.<sup>3–9</sup> Use of a navigation system also increases the accuracy of the placement of implants in joint arthroplastic surgery,<sup>10</sup> deformed long bone osteotomy, and high tibial osteotomy. Such navigation systems provide 3-dimensional (3D) information, which allows the surgeon to correct the deformity more precisely.<sup>11–13</sup> A navigation system increases the surgical accuracy by providing precise real-time information to the surgeon about the intraoperative orientation and localization. Although precise 3D information is required during a spinal osteotomy to decrease the neurovascular complications, there are few reports on the application of a navigation system in this type of operation.<sup>14,15</sup>

In the current study, we describe the successful operations using 3D spinal osteotomy on 4 complex patients, including 3 patients with a malignant tumor and 1 with spinal deformity, under the guidance of a computer-assisted navigation system. The aim of this article is to describe the surgical technique and the usefulness of computer-assisted surgery for spinal osteotomy.

### Materials and Methods

Three patients with malignant spinal tumors, which included metastatic hepatocellular carcinoma, chondrosarcoma, and fibrosarcoma, and 1 patient with a fixed kyphotic deformity as a result of ankylosing spondylitis were treated surgically using a spinal osteotomy. The level of osteotomy was the thoracic spine in 2 patients and the lumbar spine in 2 patients. The patients' preoperative demographic data are summarized in Table 1.

### Computer-Assisted Technique

The navigation system used in this study was the StealthStation TRIA (Medtronic Sofamor Danek, Memphis, TN). The navigation system comprised a computer workstation, reference frame with passive markers, standard probe, and electro-optical camera connected to the computer workstation, which served as a position sensor. The basic data used for navigation included the preoperative computed tomography (CT) imaging data (slice thickness, 1 mm). The data were transferred and recorded on the system computer and reconstructed into 3D images. The registration procedures of the point merging and surface merging produced 3D spinal images on the monitor that were identical to the actual appearance of the spine in the operative field.

After exposing the posterior element, the reference frame of the navigation system was mounted on the exposed spinous process. In cases involving an unfamiliar operative position,

From the \*Department of Orthopaedic Surgery, Graduate School of Medicine, Kyoto University, Kyoto, Japan; and †Department of Tissue Regeneration, Institute for Frontier Medical Sciences, Kyoto University, Kyoto, Japan.

Acknowledgment date: July 10, 2009. First revision date: December 9, 2009. Second revision date: February 7, 2010. Acceptance date: February 8, 2010.

The manuscript submitted does not contain information about medical device(s)/drug(s).

No funds were received in support of this work. No benefits in any form have been or will be received from a commercial party related directly or indirectly to the subject of this manuscript.

Address correspondence and reprint requests to Shunsuke Fujibayashi, MD, PhD, Department of Orthopaedic Surgery, Graduate School of Medicine, Kyoto University, 54 Shogoin Kawahara-cho, Sakyo-ku, Kyoto 606-8507, Japan; E-mail: shfuji@kuhp.kyoto-u.ac.jp

**Table 1. Summary of Patients' Demographic Data**

Case	Age	Sex	Pathology	Level for Osteotomy	Symptom	Operative Plan
1	63	M	HCC metastasis	T12	None	<i>En bloc</i> tumor resection
2	31	M	Chondrosarcoma	L4	Low back pain	<i>En bloc</i> tumor resection
3	25	F	Fibrosarcoma	T4 and T6	Back pain	Total <i>en bloc</i> spondylectomy
4	35	M	Ankylosing spondylitis	L3	Back pain and kyphosis	Posterior closing wedge osteotomy

HCC indicates hepatocellular carcinoma.

such as the lateral decubitus position, pedicle screws were placed under the assistance of the navigation system. The precise localization of the starting point and the direction of vertebral osteotomy were confirmed by the navigation system. The surgeon can check the real-time localization and the direction of the pointer tip on several 2D and 3D views on the computer screen.

Spinal osteotomy was performed using an osteotome with step-by-step confirmation of the tip position of the osteotome by the navigation system. At the same time, the navigation system provided useful anatomic information during the blind maneuver around the neurovascular structures behind the tumor or close to the vertebral body, which decreased the risk for neurovascular injury. In cases involving combined osteotomy from both the anterior and posterior approaches, it was important to keep the reference frame on the spinous process for navigating during the posterior and anterior procedures.

### Case Studies

**Case 1.** The patient was a 63-year-old man with metastasis of hepatocellular carcinoma without symptoms. The original lesions of the hepatocellular carcinoma were resolved completely after nonoperative treatments such as transcatheter arterial embolization and chemotherapy. An asymptomatic solitary metastatic lesion adjacent to the T12 vertebral body was recognized on a magnetic resonance (MR) image at the 2-year follow-up after resolution of the hepatic tumor (Figure 1). The general condition of the patient was good. Other metastatic lesions were not recognized in whole-body CT, scintigraphy, or <sup>18</sup>F-fluorodeoxyglucose positron emission tomography, and curative treatment for the metastatic lesion was advocated.

*En bloc* tumor resection to include the lateral part of the T12 vertebral body, proximal part of the 12th rib, and surrounding soft tissue through a single posterior approach was scheduled. Under general anesthesia, the patient was placed on the operation table in a right lateral decubitus position. Pedicle screws were placed from right T11 to L1 and left T11 to L1 without difficulty under the assistance of the navigation system. The assistance of the navigation system was useful for precise pedicle screw placement in the unfamiliar operative position. After the left-side hemilaminectomy and the total excision of the facet joints from T11 to L1, the left 11th and 12th spinal roots were cut under ligation. A spinal osteotomy was performed using an osteotome with step-by-step confirmation of the tip position of the osteotome by the navigation system (Figure 2A). Another skin incision was made along the left 11th rib. After the excision of the 11th rib, the anterior part of the tumor was exposed through extrapleural and retroperitoneal approaches. At this point, it was decided to cut a portion of the 12th rib with a safety margin under the guidance of the navigation system. After mapping out the starting point of the vertebral osteotomy from the anterior side, the anterior and end-

ing points of the posterior vertebral osteotomy were connected (Figure 2B). After blunt dissection of the paravertebral muscle with a safety margin under the guidance of the navigation system, the lateral aspect of the vertebral body, tumor, and proximal portion of the 12th rib were removed *en bloc* without tumor exposure. Interbody fusions using a titanium cage with harvested 11th rib grafting and posterior instrumentation were completed.

The operating time was 377 minutes, and the estimated intraoperative blood loss was 1620 mL. The postoperative course was uneventful. The patient was allowed to ambulate beginning on the first day after surgery. Postoperative CT revealed the precise osteotomy and instrumentation (Figure 3). Pathologic analysis confirmed *en bloc* tumor resection without exposure. At 1 year after the surgery, the patient reported no complaints, there was no local recurrence, and the spinal construct was solid radiologically.

**Case 2.** The patient was a 31-year-old man who complained of lower back pain caused by a huge tumor at L4. Diagnosis of chondrosarcoma was confirmed by a preoperative open biopsy at another institute. CT and MR imaging showed a huge bone tumor possibly originating from the transverse process of L4 and extending into the paravertebral muscles (Figure 4). Preoperative systemic evaluation confirmed the localized lesion

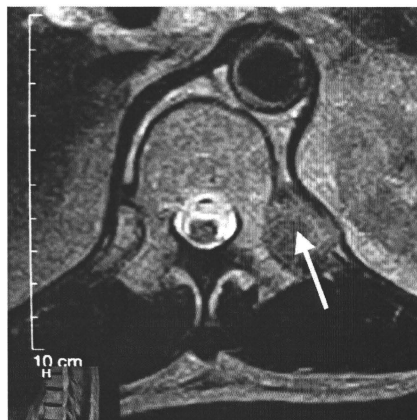


Figure 1. Case 1. Preoperative MR axial image demonstrating the solitary metastatic lesion adjacent to the T12 vertebral body. The arrow indicates the tumor.

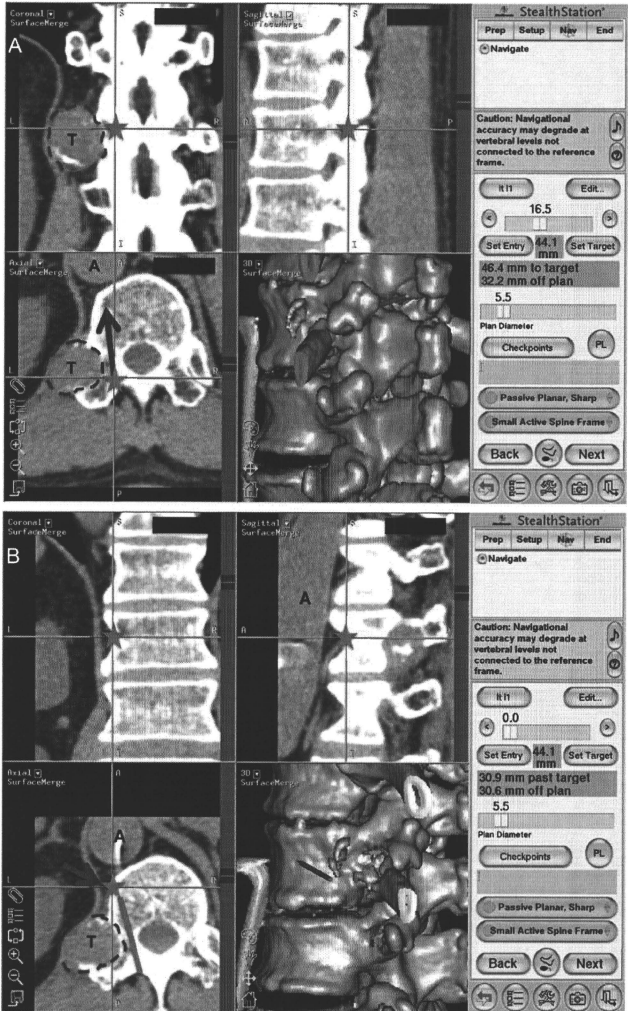


Figure 2. Case 1. The navigation system's views provide 3-dimensional, coronal, parasagittal, and axial images in conjunction with the actual instrument tip image. **A**, Pointer tip mapping of the starting point of the osteotomy from the posterior direction (asterisk). The arrow indicates the planned osteotomy from the posterior direction. The dotted line indicates the tumor margin. **B**, Pointer tip mapping of the starting point of the osteotomy from the anterior direction (asterisk). The arrow indicates the direction of the osteotomy from the anterior direction, which connects to the ending point of the osteotomy from the posterior direction. T indicates tumor; A, aorta.

without metastasis. A curative operation was planned to involve an *en bloc* tumor resection combined with the right half of the L4 vertebral body. Computer-assisted spinal osteotomy and *en bloc* tumor resection were performed through the combined anterior and posterior exposure as described in case 1 (Figure 5).

The right L2–L4 nerve roots were involved in the huge tumor and were killed. The osteotomized vertebral body, huge tumor, and paravertebral muscle were removed *en bloc* with-

out tumor exposure. Spinal reconstruction with a titanium cage with autogenous iliac crest bone graft and anteroposterior instrumentation from L2 to S1 was performed. An incidental dural tear was repaired successfully. The operating time was 999 minutes, and the estimated intraoperative blood loss was 7000 mL. Postoperative CT demonstrated complete resection of the tumor and a precise osteotomy of the right half of the vertebral body and reconstruction using the titanium cage (Figure 4). Pathologic analysis revealed complete excision of the

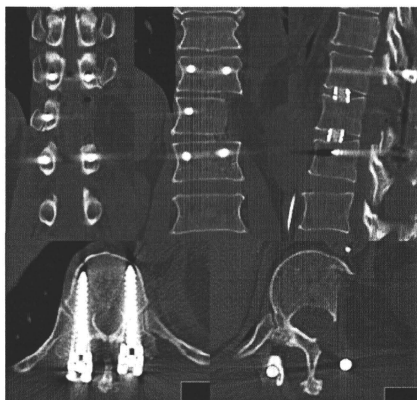


Figure 3. Case 1. Postoperative CT images demonstrating the precise osteotomy, *en bloc* tumor excision, and accurate pedicle screw placement.

huge tumor without exposure on the osteotomy line. Although right leg paresis occurred as a result of the intentional nerve root sacrifice, the patient could ambulate with one cane. Bony union was achieved through the cage 1 year after the surgery (Figure 6). Although no local recurrence was observed at the 2-year follow-up, the patient died from lung metastasis 3 years after the surgery.

**Case 3.** The patient was a 25-year-old woman who complained of severe back pain caused by a pathologic fracture at T5. Diagnosis of fibrosarcoma was defined by a preoperative needle biopsy. CT and MR imaging demonstrated a pathologic fracture and epidural tumor extension from caudal T4 to cranial T6, which compressed the spinal cord severely (Figure 7).

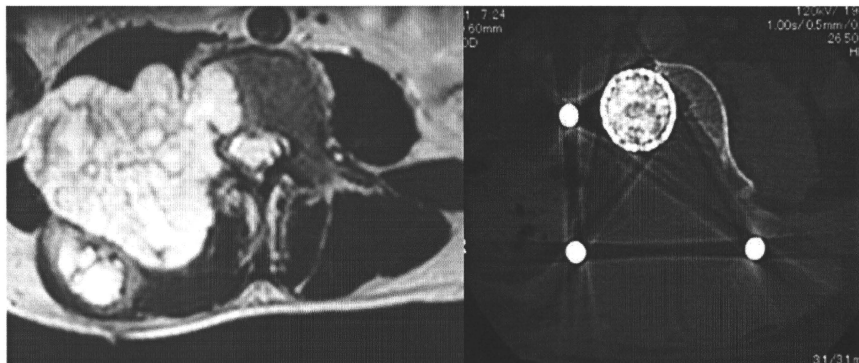


Figure 4. Case 2. Comparison of preoperative MR axial image (left) and postoperative (right) CT axial image. The images demonstrate the precise *en bloc* excision of a large tumor by spinal osteotomy and reconstruction using a titanium mesh cage with an autogenous bone graft.

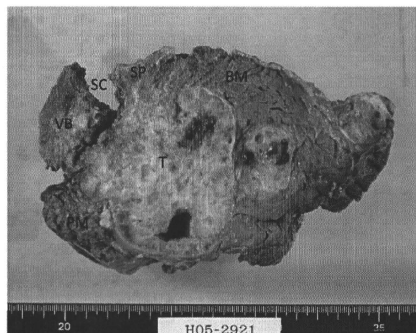


Figure 5. Case 2. Photograph of cross section of the *en bloc* specimen after removal. VB indicates vertebral body; T, paravertebral tumor; SC, spinal canal; SP, spinous process; BM, back muscle; PM, psoas muscle.

Preoperative whole-body examination confirmed a solitary lesion without metastasis. A total *en bloc* spondylectomy from caudal T4 to cranial T6 was scheduled. A computer-assisted spinal osteotomy using a T-saw and total *en bloc* spondylectomy were performed through a single posterior exposure. The safety margin of the spinal osteotomy and the relationship with the surrounding neurovascular structures were confirmed at each step of the operation using the navigation system. The navigation system provided important anatomic information during the blind maneuver around the anterior aspect of the vertebral body.

After the *en bloc* spondylectomy, spinal reconstruction with a titanium cage with an autogenous iliac crest bone graft and posterior instrumentation from T3 to T8 were performed. The operating time was 495 minutes, and the estimated intraoperative blood loss was 1640 mL. Pathologic analysis revealed complete resection of the tumor without exposure. A postop-



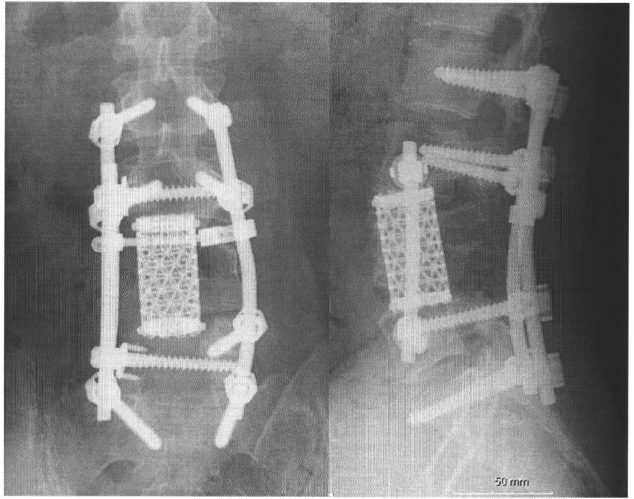


Figure 6. Case 2. Anteroposterior and lateral radiographs at the 1-year postoperative follow-up showing spinal reconstruction after *en bloc* tumor resection and solid bony union.

erative CT demonstrated the precise osteotomy and spinal reconstruction using the titanium cage (Figure 7). The postoperative course was uneventful, and the patient underwent adjuvant chemotherapy. One year after surgery, radiologic examination showed good bony union through the cage and no local recurrence (Figure 8).

**Case 4.** The patient was a 35-year-old man who complained of back pain and a severe kyphotic posture that prevented him from looking forward and maintaining the supine position, which restricted his daily activities severely. Ankylosing spondylitis was diagnosed as “bamboo spine,” and the patient was HLA-B27 positive and had elevated C-reactive protein concentration. Kyphosis was 77° caused by the combination of 48° at the thoracic spine (T1–T12) and 29° at the lumbar spine (L1–L5) (Figure 9). A C7 plumb line was shifted 27.9 cm anteriorly

to the sacral promontory, and the chin-brow vertical angle (CBVA) was 54° (Figure 10A).<sup>16</sup> We scheduled a 45° posterior-closing wedge spinal osteotomy at the L3 vertebra and posterior instrumentation from T12 to L5. The degree of spinal osteotomy and the relationship with surrounding neurovascular structures were confirmed at each step of the operation using the navigation system. A temporary rod was attached to the pedicle screws across to the osteotomy to avoid sudden movement. The osteotomized site was closed successfully using a bending maneuver on a flexible operating table and gradual compression with instrumentation. Postoperative lateral radiograph and CT revealed a 44° osteotomy (Figure 9), which corrected the lumbar lordosis to 15°, the anterior shift of the C7 plumb line to 5.4 cm, and the CBVA to 9° (Figure 10B). The operating time was 421 minutes, and the estimated intraoperative blood loss was 536 mL. After the operation, the patient

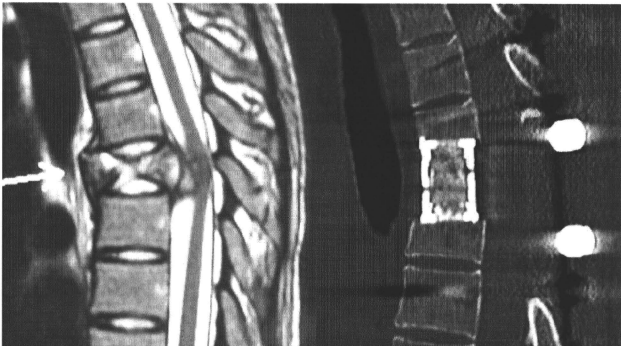


Figure 7. Case 3. Comparison of preoperative MR sagittal image (left) and postoperative (right) CT sagittal image. The images demonstrate the precise total *en bloc* spondylectomy from caudal T4 to cranial T6 by spinal osteotomy and reconstruction using a titanium mesh cage with an autogenous bone graft.

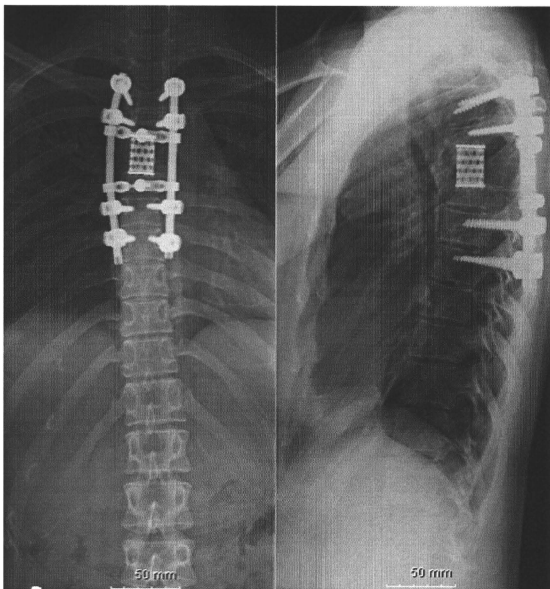


Figure 8. Case 3. Anteroposterior and lateral radiograph of the thoracic spine at the 1-year postoperative follow-up showing restoration of the sagittal alignment after *en bloc* tumor resection and solid bony union.

could look forward and maintain a supine position, and his back pain resolved. Successful bony union at the osteotomized site was achieved 6 months after the operation, and sagittal alignment was well maintained at the 1-year follow-up.

### ■ Results and Discussion

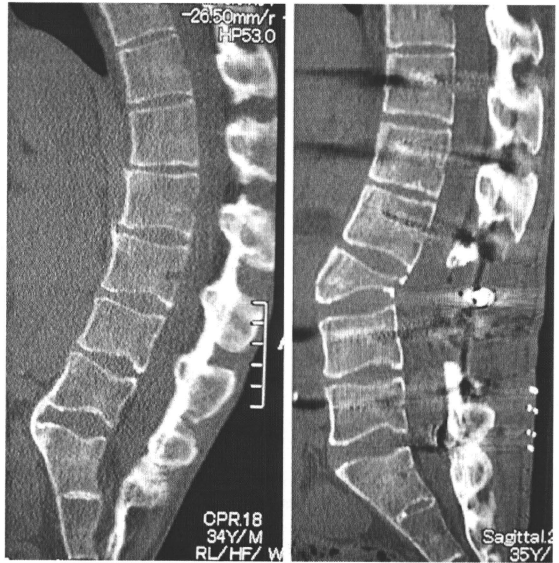
In all 4 patients, 3D spinal osteotomy was performed successfully. The computer-assisted navigation system was useful for mapping the osteotomy site and surrounding tissues intraoperatively in every patient. Postoperative radiograph and CT confirmed the precise osteotomy, implant placement, and deformity correction according to the preoperative plan. Pathologic analysis also showed *en bloc* tumor resection without tumor exposure on the osteotomy line in all 3 tumor cases. The results of the operative procedure are summarized in Table 2.

Computer-assisted surgery, using a CT-based navigation system, has been introduced successfully to facilitate highly accurate surgical procedures in spinal surgery. The operative field and preoperative images are combined by registration, or integration, of the preoperative imaging methods within the surgical environment. The accuracy and usefulness of a navigation system in the placement of pedicle screws are recognized and have been discussed. Numerous comparative studies have demonstrated the increased accuracy of pedicle screw placement for several spinal disorders including cervical and scoliosis surgery.<sup>17,18</sup>

Other applications of the navigation system include the excision of spinal pathologies, including osteoid osteoma, hemangioma, chordoma, ossification of the posterior longitudinal ligament, and ossification of the ligamentum flavum.<sup>3-9</sup> The navigation system provides the information needed to excise the lesion completely without causing neurovascular injury to the surrounding tissues.

We think other good candidates for navigation surgery are 3D deformity correction and *en bloc* tumor resection, which require a precise osteotomy and excision according to the preoperative planning. In such complex anatomic pathologies, even skillful and experienced surgeons can lose the localization and orientation during the operation, which can lead to poor surgical results and complications. Spinal osteotomy is a complex surgery involving the wide resection of a malignant tumor *en bloc* or correction of a fixed spinal deformity. The problems for conventional spinal osteotomy include the blind maneuver around the spinal cord, nerve root, and major vessels, and the potential for incorrect or insufficient osteotomy, tumor exposure during incorrect osteotomy, insufficient correction of a spinal deformity, or nonunion after the corrective osteotomy. A rigid spinal deformity such as ankylosing spondylitis does not have a compensatory mechanism, and precise osteotomy and correction are required. We performed a precise osteotomy for each

Figure 9. Case 4. Comparison of preoperative (left) and postoperative (right) CT sagittal images. The images demonstrate the precise osteotomy at L3 and correction of the ankylosing spondylitis deformity.



patient according to preoperative planning, and the follow-up showed that successful postoperative sagittal alignment and early bony union were achieved. In patients with a solitary malignant tumor in the spine, *en bloc* resection with a safety margin, such as a total *en bloc* spondylectomy, is mandatory to provide a curative treatment.<sup>19-21</sup>

In all our tumor patients, total resection with a safety margin was the best procedure. In general, total resection for such lesions requires combined anterior and posterior approaches, and a very invasive operation. In patients 1 and 3, using the navigation system allowed the operations to be performed in single stages without the need to change the patient's position, which decreased the surgi-

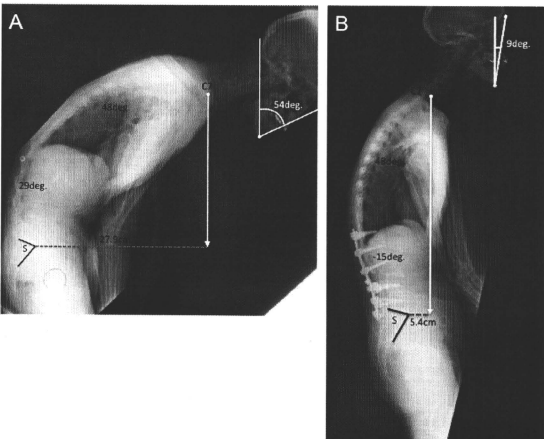


Figure 10. Case 4. Comparison of preoperative (A) and postoperative (B) full-length lateral radiographs. Lumbar lordosis, anterior shift of the C7 plumb line, and CBVA were corrected from 29° of kyphosis, 27.9 cm, and 54° to -15° of kyphosis, 5.4 cm, and 9°, respectively.

**Table 2. Summary of Postoperative Clinical Data**

Case	Operative Time (min)	Blood Loss (mL)	% EBV*	Operative Procedure	Complications
1	377	1620	32.2	<i>En bloc</i> tumor resection, Posterior interbody fusion (T11–L1)	None
2	999	7000	156.6	<i>En bloc</i> tumor resection, Anteroposterior spinal fusion (L2–S)	Dural tear and right leg paresis†
3	495	1640	54.8	Total <i>en bloc</i> spondylectomy, Posterior spinal fusion (T3–T8)	None
4	421	536	13.0	Closing wedge osteotomy, Posterior spinal fusion (T12–L5)	None

Average blood volume = 75 mL/kg in adult men, 65 mL/kg in adult women.  
% EBV = blood loss/EBV [times] 100.

\*EBV (estimated blood volume) = weight (kg) [times] average blood volume.  
†Right leg paresis caused by intentional right L2–L4 nerve root sacrifice.

cal invasiveness and decreased the operating time. The navigation system allows the optimal anteroposterior, mediolateral, and rostral-caudal trajectories of the osteotomy selected in the virtual model to be replicated intraoperatively. Thus, a safe 3D osteotomy can be performed with the optimal amount and orientation of correction, which increases the safety of the neural and vascular structures. In addition, we estimate that both the patient and surgeon receive less radiation exposure than if standard fluoroscopy is used.

Another major advantage of navigation surgery is the feasibility of virtual surgery and practicing the operative plan before surgery. The surgeon can experience virtual surgery several times on the computer screen using 2D- and 3D-reconstructed CT images, which provide the important anatomic information to the surgeon before the operation, and facilitate the safety and accuracy of the operation in the real operative theater.

The disadvantage of existing CT-based navigation systems is the difficulty in navigating the anatomically flat structures such as the anterior spine and postlaminectomy spine. In such situations, setting the reference frame and accomplishing the surface registration are difficult. The usefulness of image-assisted surgery using intraoperative CT for multioperated complex deformity surgery was reported recently.<sup>14</sup> Such new technology will provide a less invasive, safer, and more accurate surgery. In addition, the instrumented spine is difficult to navigate because of the artifact related to the metal implants. In the clinical arena, salvage surgeries are often required for such complex pathologies, and development of novel navigation systems is required to solve such problems.

Because this is a technical note, and the sample size and follow-up periods were limited, it was difficult to compare the obvious advantages of computer-assisted surgery with conventional fluoroscopy-guided surgery in terms of the long-term clinically relevant outcomes. The use of a computer-assisted navigation system will help ensure the safety and efficacy of a complex 3D spinal osteotomy.

#### ■ Key Points

- The surgical technique and usefulness of computer-assisted surgery for spinal osteotomy are presented.

- Four complex cases, including 3 solitary malignant spinal tumors and 1 spinal kyphotic deformity of ankylosing spondylitis, were treated surgically using a computer-assisted navigation system.
- The navigation system provided useful real-time information to the surgeon during the osteotomy surgery; this information included the precise localization and orientation of the tumor or deformity.

#### References

- Kosmopoulos V, Schizas C. Pedicle screw placement accuracy: a meta-analysis. *Spine* 2007;32:E111–20.
- Rajasekaran S, Vidyadhara S, Ramesh P, et al. Randomized clinical study to compare the accuracy of navigated and non-navigated thoracic pedicle screws in deformity correction surgeries. *Spine* 2007;32:E56–64.
- Arand M, Hartwig E, Kinzl L, et al. Spinal navigation in tumor surgery of the thoracic spine: first clinical results. *Clin Orthop Relat Res* 2002;398:211–8.
- Neo M, Asato R, Honda K, et al. Transmaxillary and transmandibular approach to a C1 chordoma. *Spine* 2007;32:E236–9.
- Rajasekaran S, Vijay K, Shetty AP. Intraoperative Iso-C three-dimensional navigation in excision of spinal osteoid osteomas. *Spine* 2008;33:E25–9.
- Sakanishi H, Hoshi K, Nakajima S, et al. Vertebral hemangiomas compressing the thoracic spinal cord: application of computer-aided navigation and intraoperative spinal sonography for surgery through anterior and posterior approaches. *J Orthop Sci* 2006;11:294–7.
- Seichi A, Nakajima S, Takeshita K, et al. Image-guided resection for thoracic ossification of the ligamentum flavum. *J Neurosurg* 2003;99(suppl 1):60–3.
- Seichi A, Takeshita K, Kawaguchi H, et al. Image-guided surgery for thoracic ossification of the posterior longitudinal ligament. Technical note. *J Neurosurg* 2005;3:165–8.
- Van Royen BJ, Baayen JC, Pijpers R, et al. Osteoid osteoma of the spine: a novel technique using combined computer-assisted and gamma probe-guided high-speed intralesional drill excision. *Spine* 2005;30:369–73.
- Stulberg SD, Beng PL, Sarin V. Computer-assisted navigation in total knee replacement: results of an initial experience in thirty-five patients. *J Bone Joint Surg Am* 2002;84:90–8.
- Gregg RK, Matthew SA, Smith EB, et al. Total knee arthroplasty using computer-assisted navigation in patients with deformities of the femur and tibia. *J Arthroplasty* 2006;21:284–8.
- Jackson DW, Warkentine B. Technical aspects of computer-assisted opening wedge high tibial osteotomy. *J Knee Surg* 2007;20:134–41.
- Keppler P, Gebhard F, Grutzner PA, et al. Computer-aided high tibial open wedge osteotomy. *Injury* 2004;35(suppl 1):S A68–78.
- Metz LN, Burch S. Computer-assisted surgical planning and image-guided surgical navigation in refractory adult scoliosis surgery case report and review of the literature. *Spine* 2008;33:E287–92.
- Ohmori K, Kawaguchi Y, Kanamori M, et al. Image-guided anterior thoracolumbar corpectomy: a report of three cases. *Spine* 2001;26:1197–201.
- Suk KS, Kim KT, Lee SH, et al. Significance of chin-brow vertical angle in correction of kyphotic deformity of ankylosing spondylitis patients. *Spine* 2003;28:2001–5.

17. Kotani Y, Abumi K, Ito M, et al. Improved accuracy of computer-assisted cervical pedicle screw insertion. *J Neurosurg* 2003;99(suppl 3):257-63.
18. Kotani Y, Abumi K, Ito M, et al. Accuracy analysis of pedicle screw placement in posterior scoliosis surgery comparison between conventional fluoroscopic and computer-assisted technique. *Spine* 2007;32:1543-50.
19. Melcher I, Disch AC, Khodadadyan-Klostermann C, et al. Primary malignant bone tumors and solitary metastases of the thoracolumbar spine: results by management with total en bloc spondylectomy. *Eur Spine J* 2007;16:1193-202.
20. Sakaura H, Hosono N, Mukai Y, et al. Outcome of total en bloc spondylectomy for solitary metastasis of thoracolumbar spine. *J Spinal Disord Tech* 2004;17:297-300.
21. Tomita K, Kawahara N, Baba H, et al. Total en bloc spondylectomy for solitary spinal metastases. *Int Orthop* 1994;18:291-8.

## Advantages of the Paraspinal Muscle Splitting Approach in Comparison With Conventional Midline Approach for S1 Pedicle Screw Placement

Masato Ota, MD, Masashi Neo, MD, PhD, Shunsuke Fujibayashi, MD, PhD,  
Mitsuru Takemoto, MD, PhD, and Takashi Nakamura, MD, PhD

**Study Design.** A retrospective comparative study of the S1 pedicle screw (S1PS) position obtained using 2 surgical approaches.

**Objective.** To determine whether the paraspinal approach leads to more medially oriented placement of the S1PS compared with the midline approach.

**Summary of Background Data.** To obtain a stronger as well as safer fixation of the S1PS, medially oriented screw placement is very important. However, no study has recommended a surgical approach to achieve this object.

**Methods.** The positions of 32 screws placed by the midline approach and 34 screws placed by the paraspinal approach were compared using postoperative computed tomography. The location of the bilateral common iliac veins (CIV) in relation to the S1PS tips was also analyzed to evaluate their safety.

**Results.** There was no statistical difference in screw insertion point regardless of the approach employed. However, in the paraspinal group the S1PS were placed with significantly greater medial direction and with longer screws. In addition, they pierced the anterior sacral cortex closer to the midline compared with the midline approach. Four left screws in the midline approach group made contact with the left CIV, whereas no screw in the paraspinal approach group lay adjacent to the CIV.

**Conclusion.** Our results demonstrate that the paraspinal approach for S1PS placement may be superior to the midline approach in terms of the medially oriented screw placement that is biomechanically stronger and less risky for the CIV.

**Key words:** sacral screw fixation, paraspinal approach, pedicle screw, complication, mechanical strength. *Spine* 2010;35:E452–E457

Pedicle screw fixation in the lumbar spine has been relatively successful, but S1 pedicle screw (S1PS) fixation remains a challenging clinical problem. Despite efforts to develop a stable S1PS fixation technique, a high incidence of instrumentation failure and pseudarthrosis continue to plague the procedure.<sup>1,2</sup> Problems of S1PS fixa-

tion, particularly with the placement of the S1PS without supplemental distal fixation, are attributable to not only biologic but also mechanical factors of the sacrum. These factors include low bone mineral density of the sacrum, difficulty in obtaining an appropriate direction of the S1PS, large cantilever bending forces being applied to the distal instrumentation, and the difficulty in access to, and visualization of, the starting point of the S1PS.<sup>3</sup> To overcome these disadvantages, alternative fixation techniques, such as posterior sacral fixation with iliac fixation, combination of S1PS with a sacral alar screw or hooks, or an S2PS have been proposed.<sup>4</sup> However, increasing the range of internal fixations may give rise to instrument-related complications, and fixations into the ilium may create disorders of the sacroiliac joint.<sup>5</sup>

It is essential, therefore, that techniques for the placement of S1PS to achieve ideal sacral purchase should be established. A variety of studies regarding biomechanical evaluations of S1PS orientation as well as screw purchase in the anterior sacral cortex have been investigated previously.<sup>6–15</sup> In particular, the S1PS orientation should be considered. Convergence of the PSs produces a triangulation effect that should substantially increase the pullout strength of a fully assembled construct. Barber *et al* verified that compared with those placed in parallel, paired PSs placed at 30 degrees of convergence in the lumbar spine sustained a statistically higher load at the threshold of loosening.<sup>14</sup> Furthermore, it is generally agreed that medially oriented placement of the S1PS provides greater stability than either straight-ahead or laterally oriented positions, because the mean bone mineral density in the central region of the sacrum was found to be approximately 30% to 60% higher than in the alar region.<sup>12,13</sup> Peretti *et al*, in their cadaveric study showed that S1PS with an inward obliquity of 10 degrees had 43% greater resistance to pullout forces than those with a straight-ahead position.<sup>7</sup> Similarly, Zheng *et al* clarified that the insertion torque of medially directed S1PS was 42% to 101% higher than that of laterally directed S1PS.<sup>13</sup> Thus, it seems that medially oriented S1PS placement is necessary to obtain a secure anchor to the sacrum.

Bicortical screw fixation also increases the mechanical strength of a S1PS.<sup>10,13</sup> In this case, however, knowledge of the neurovascular structures anterior to the sacrum is very important. Not only excessive penetration of the ventral sacral cortex but also far lateral screw penetration potentially carries greater risks to the neurovascular structures such as the iliac vessels and the lumbosacral

From the Department of Orthopaedic Surgery, Graduate School of Medicine, Kyoto University, Kyoto, Japan.

Acknowledgment date: August 4, 2009. Revision date: September 29, 2009. Acceptance date: November 3, 2009.

The device(s)/drug(s) is/are FDA-approved or approved by corresponding national agency for this indication.

No funds were received in support of this work. No benefits in any form have been or will be received from a commercial party related directly or indirectly to the subject of this manuscript.

Address correspondence and reprint requests to Masato Ota, MD, Department of Orthopaedic Surgery, Graduate School of Medicine, Kyoto University, 54 Kawahara-cho, Shogoin, Sakyo-ku, Kyoto 606-8507, Japan; E-mail: otamasa@kuhp.kyoto-u.ac.jp

trunk.<sup>16-19</sup> Although, fortunately, a fatal case has never been reported, Ergur *et al* reported that injuries of the lumbosacral trunk could cause neurologic deficit or chronic pain.<sup>18</sup> To avoid these complications, an adequate medial orientation of the S1PS is necessary.

Considering the combination of biomechanical advantages and anatomic safety, a S1PS placement as medially oriented as possible is desirable. However, no study has yet addressed the best surgical approach to permit medially oriented placement of the S1PS screws. The purpose of this study was to investigate whether a paraspinal muscle-splitting approach leads to more medially oriented placement of the S1PS compared with the conventional midline approach. In addition, we attempted to examine the location of the common iliac vein (CIV) to assess the safety of anterior sacral structures.

## ■ Materials and Methods

### Patient Population

A total of 68 S1PS were placed in 34 patients with degenerative disorders who underwent lumbosacral fixation at our institution between May 2001 and May 2008, and who were examined with postoperative computed tomography (CT) imaging. Patients with infections, tumors, or previous lumbosacral surgery were excluded from this study. To compare 2 surgical approaches for S1PS placement, the subjects were classified into 2 groups. Of the 68 screws, 32 S1PS in 16 patients were inserted by the conventional midline approach up to June 2005, whereas 36 S1PS in 18 patients were inserted using the paraspinal muscle-splitting approach described by Wiltse *et al*<sup>20</sup> from July 2005 onward. To harvest massive bone graft, the bilateral posterior superior iliac spine was resected in only 1 case with the paraspinal approach, and it was excluded from this study. Consequently, the midline approach group consisted of 32 S1PS in 16 patients and the paraspinal approach group consisted of 34 S1PS in 17 patients.

The demographic characteristics of the patients in these groups including age, gender, preoperative diagnosis, fusion level, and surgical method for lumbosacral fusion are listed in Table 1. The original diagnoses in both groups were diverse lumbosacral degenerative disorders as shown in Table 1.

### Surgical Procedures for S1PS Placement

In both approaches, a midline posterior skin incision was made. In the midline approach, the deep fascia was incised in the middle, and the multifidus muscles were subsequently freed from spinous processes and lamina attachments to the lateral aspect of the L5/S1 facet joint by conventional techniques. However, in the paraspinal approach the paramedian fascial incisions were made in their correct place, which was usually located 2 to 3 cm lateral to the midline. After the natural cleavage plane of the anatomic intermuscular space between multifidus and longissimus muscles was identified, a muscle-splitting technique using blunt finger dissection between these muscles could be used to gain access to the lateral parts of the L5/S1 facet joint. In both approaches, our entrance point for the S1PS insertion was the inferolateral corner of the S1 superior articular process. Orientation of the screw axis was aimed as medially as possible to a sacral midline in the horizontal plane. The posterior superior iliac spine was not resected. In the sagittal plane, the sacral promontory was located under lateral fluoro-

**Table 1. Patient Demographic Data**

	Midline Approach Group	Paraspinal Approach Group	P
No. patients	16	17	
No. S1 pedicle screws	32	34	
Mean age at surgery ( $\pm$ SD)	53.3 $\pm$ 20.6	46.6 $\pm$ 17.6	0.2639*
Gender (male/female) (% male)	10/6 (62.5)	12/5 (70.6)	0.6223†
Preoperative diagnosis (% of patients)			
Degenerative spondylolisthesis	5 (31.3)	2 (11.8)	
Isthmic spondylolisthesis	4 (25)	6 (35.3)	
Degenerative disc disease	2 (12.5)	3 (17.6)	
Recurrent disc hernia	3 (18.8)	2 (11.8)	
Intraforaminal disc hernia	1 (6.3)	2 (11.8)	
Other conditions	1 (6.3)	2 (11.8)	
Level of fusion (% of patients)			
One level (L5/S1)	11 (68.8)	15 (88.2)	
Two levels (L4-S1)	3 (18.8)	2 (11.8)	
Three levels (L3-S1)	1 (6.3)	0	
Four levels (L2-S1)	1 (6.3)	0	
Surgical method for L5/S1 fusion (% of patients)			
Transformaminal lumbar interbody fusion	10 (62.5)	16 (94.1)	
Posterior lumbar interbody fusion	6 (37.5)	1 (5.9)	

\*Mann-Whitney U test.

† $\chi^2$  for independence test.

scopic guidance. We aimed for secure fixation by pinching the screw tip between the anterior and superior cortices of the sacral promontory. However, when the surgeon wanted more secure fixation the anterior sacral cortex was carefully penetrated by a pedicle probe or an awl. To obtain a bicortical fixation of the screw, we chose a screw that was 0 to 5 mm longer than the measured depth to the anterior cortex. After the pathway was inspected with a sounder for any bone breaches, the S1PS was inserted with the identical trajectory.

All screws were placed by 1 of 3 senior authors or under their supervision. Eleven types of PS systems were used in this study. The selection of the PS type was at the surgeon's discretion.

### Assessment Using CT

A postoperative CT scan was routinely performed within a few weeks of surgery for all patients to confirm whether the graft bone or interbody cages, as well as the PSs, had been implanted in the correct position. Three different types of CT scanner were used in this series: the Lemage Supreme (GE Yokogawa Medical Systems, Tokyo, Japan), HiSpeed QX/i (GE Yokogawa Medical Systems, Tokyo, Japan), and Aquilion64 (Toshiba Medical Systems, Tokyo, Japan). Horizontal slices along the S1PS axis were cut to a slice thickness of 2 to 3 mm and a slice interval of 2 to 3 mm in all cases. The best slice close to the center of the screw was selected to evaluate the position of the S1PS and the location of the CIV anterior to the sacrum on both sides, as follows.

First, we measured from the CT images for all 66 S1PS the distance from the anteroposterior sacral vertebral midline to the midpoint of the screw at the posterior cortical insertion point (IPD), the S1PS angle (PSA), which was defined as the angle between the screw axis and the midline, the S1PS length (PSL), which was defined as the distance between the screw midpoints at the IPD and the anterior cortical penetration point, and the distance from the midline to the lateral edge of

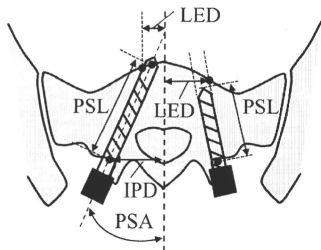


Figure 1. Illustration of the measurements made of the S1 pedicle screw (S1PS) position. IPD indicates distance from the vertebral midline to the screw insertion point; PSA, S1PS angle; PSL, length of S1PS length within the sacral body; LED, distance from the midline to the lateral edge of the screw perforation at the anterior sacral cortex. The right side screw of the illustration shows the method of measurement of PSL and LED when the screw did not reach the anterior cortex.

the S1PS perforation of the anterior sacral cortex (LED) (Figure 1). When the S1PS did not reach the anterior sacral cortex, PSL was measured as the distance from the screw tip to the IPD. LED was also defined as the distance from the midline to the cross-point of the extension of the lateral edge of the screw and the anterior cortex as shown in Figure 1.

Second, to compare the anatomic locations of bilateral CIVs, the shortest distance from the midline to the CIV (MVD) and the shortest distance from anterior sacral cortex to the CIV (SVD) were measured (Figure 2). For these assessments, we decided on the correct position of the CIV after referring to several cranial CT images which were traced back to the level of divergence of the inferior vena cava. Only 26 screws (13 images) in the midline approach group and 30 screws (15 images) in the parasagittal approach group were eligible, because for 3 images in the former group and 2 in the latter it was difficult to precisely confirm the contour of the CIV. When the S1PS protruded anterior to the sacral anterior cortex we also measured for each group the number of screws that were situated <1 mm from the CIV.

All linear and angular parameters were measured with a precision of 0.5 mm and 0.5 degrees, as dictated by Centricity PACS system version 2.0 (GE healthcare, Milwaukee, WI). All records were retrospectively examined by the first author.

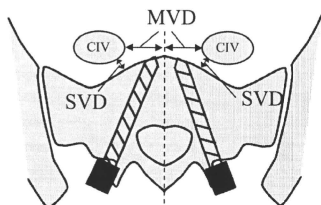


Figure 2. Illustration of measurements indicating the location of the right and left common iliac vein (CIV). MVD indicates the shortest distance from the midline to the CIV; SVD, the shortest distance from the anterior sacral cortex to the CIV.

Table 2. S1 Screw Position in the 2 Treatment Groups

	Midline Approach Group	Parasagittal Approach Group	P
No. S1 pedicle screws	32	34	
IPD (mm)	28.9 ± 2.18	30.1 ± 2.83	0.0867
PSA (degrees)	17.1 ± 6.82	23.7 ± 5.27	0.002*
PSL (mm)	43.2 ± 5.12	46.5 ± 4.44	0.029*
LED (mm)	18.9 ± 4.86	13.9 ± 7.16	0.0017*

\*P < 0.05.

IPD indicates distance from the vertebral midline to the screw insertion point; PSA, S1 pedicle screw angle; PSL, S1 pedicle screw length in the sacral body; LED, distance from the midline to the lateral edge of the screw at the anterior sacral cortex.

Statistical Analyses

The Mann-Whitney U test was performed to compare the non-parametric variables such as the S1 screw positions of the 2 groups and the CIV locations on right and left sides. The  $\chi^2$  for independence test was used for comparison of the frequencies. P < 0.05 was considered to be significant. All statistical analyses were performed using StatView software version 5.0 (SAS Institute Inc., Cary, NC).

Results

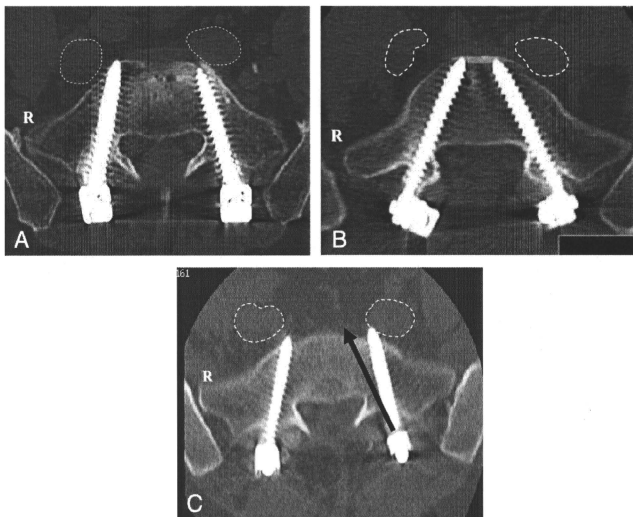
There were no significant differences in age and gender between the 2 treatment groups (Table 1). All 66 S1PS were fully contained within the cortical boundaries of the S1 pedicle and no screw was identified on CT evaluation to have breached the medial wall of the S1 pedicle. Screw diameters were 6.5 or 7.5 mm in both groups and no significant differences in screw diameters between the 2 groups were found (P = 0.1055). Twenty-one (65.6%) of 32 screws in the midline approach group penetrated the anterior sacral cortex by an average of 3.33 ± 1.86 mm whereas 18 (52.9%) of 34 screws in the parasagittal approach group penetrated by a mean of 4.11 ± 2.15 mm. Neither the number of penetrated screws nor their protruded length was significantly different between the 2 groups (P = 0.2949 and P = 0.2312, respectively).

The S1PS positions in the 2 groups, which were assessed by IPD, PSA, PSL, and LED, are summarized in Table 2. When the screw insertion point estimated by IPD was analyzed, there was no significant difference. In contrast, significant differences were found between the 2 treatment groups with respect to PSA, PSL, and LED. By the parasagittal approach, S1PS could be placed not only with a more medial orientation but also with a longer screw purchase than by the midline approach. In addition, the analysis showed that in the parasagittal approach group the S1PS pierced the anterior sacral cortex closer to the midline compared with the midline approach group (Figures 3A, B).

With respect to the anatomic location of the CIV, our results show that the MVD on the left side was significantly shorter than that on the right side. In contrast, our results show no significant difference in the SVD between the left and right sides (Table 3). Of 26 screws in the midline approach group, 4 left screws (15.4%) were vi-



Figure 3. Three representative cases illustrated on postoperative CT images. The dotted circles show the contours of the CIV. **A**, An example of the placement in the midline approach group. IPD: 28.5/29.0 mm; PSA: 11.5/15.5 degrees; PSL: 47.5/46.0 mm; LED: 21.0/16.5 mm (right and left side, respectively). **B**, An example of the placement in the paraspinal approach group. IPD: 29.0/31.0 mm; PSA: 24.0/28.5 degrees; PSL: 55.0/54.0 mm; LED: 10.0/9.5 mm (right and left side, respectively). **C**, An example from the midline approach group where the S1PS lies adjacent to the CIV. MVD: 23.0/20.0 mm and SVD: 5.5/3.5 mm (right and left side, respectively). The left S1PS is evidently in contact with the left CIV. The ideal orientation of the left screw is indicated by the black arrow.



sually in contact with the left CIV (Figure 3C). On the other hand, no screw lay adjacent to the CIV in the paraspinal approach group (Table 4).

## ■ Discussion

In recent years, the Wiltse *et al* paraspinal approach to the lumbar spine,<sup>20</sup> which was achieved by developing the plane between the multifidus and the longissimus muscles, has been revised owing to an increased enthusiasm for development of minimally invasive operating techniques.<sup>21,22</sup> Several studies suggest that this procedure minimizes the ischemia and denervation of the paraspinal musculature resulting from the detachment of muscle from the spinous processes and its subsequent prolonged wide retraction used in the conventional midline approach, which may lead to postoperative muscle atrophy and pain.<sup>23,24</sup> Moreover, this procedure easily establishes access to the lateral aspect of the L5/S1 facet joint with minimal retraction of paravertebral muscles, although a few of the most lateral fibers of the multifidus are occasionally dissected because their bulky fibers are fanning caudally over the sacrum.<sup>25</sup>

**Table 3. Location of the CIV**

	Right Side	Left Side	P
MVD (mm)	23.6 ± 5.03	19.5 ± 8.33	0.0069*
SVD (mm)	6.59 ± 4.32	5.96 ± 5.27	0.1403

\*P < 0.05.

MVD indicates the shortest distance from the midline to the CIV; SVD, the shortest distance from anterior sacral cortex to the CIV.

The present study demonstrated that it was possible to expose the optimal S1PS starting point located at the inferolateral corner of L5/S1 facet joint by both the midline and paraspinal approaches. However, in our series, the paraspinal approach provided a more medial orientation of S1PS placement. Although the midline approach managed to expose the entry point with wide retraction of the paravertebral muscles, it is likely that several factors would impede an ideal medially oriented placement of S1PS. It was pointed out that potential obstructions included a large screw head and shaft or wide instrumentation device, the prominence of the posterior iliac crest, muscle mass, and retractors.<sup>26</sup> Many authors have asserted that it is difficult to achieve a sufficiently medially oriented placement for the S1PS because of the dorsal overhang of the posterior iliac crest.<sup>7,27,28,29</sup> Kaptanoglu *et al* recommended first resecting the ilium to allow for a more medial trajectory for S1PS placement.<sup>27</sup> In the present study, the removal of the posterior superior iliac spine was not performed. Nevertheless, in the paraspinal approach group the reduction of the muscle volume impinging between the retractor and the posterior iliac crest enabled us to insert a screw with adequate medial orientation (Figure 4). From these

**Table 4. No. Screws Contact With CIV**

	Right Side	Left Side
Midline approach group (n = 26)	0	4 (15.4%)
Paraspinal approach group (n = 30)	0	0

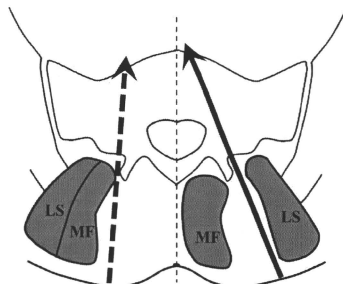


Figure 4. Schematic illustration of S1PS trajectory comparing the parasagittal and midline approaches. The arrow and dotted arrow represent the S1PS directions achieved by the parasagittal and midline approaches, respectively. MF indicates the multifidus muscle; LS, the longissimus muscle.

discussions, we stress that the parasagittal approach is particularly useful for S1PS placement in patients with either a bulky paravertebral muscle volume or a large overhang of the posterior iliac crest observed on preoperative CT or magnetic resonance imaging.

Medially oriented screw placement provides a more secure anchor to the sacrum for the 2 reasons mentioned in the Introduction, that is, the triangulation effect and the insertion of screws into denser bone. Our results, furthermore, demonstrated that the parasagittal approach gave a longer screw fixation than the midline approach, probably because of more medially oriented screw placement. Krag *et al* suggested that even a 5-mm longer screw can provide a significant increase in bone-screw fixation strength.<sup>30</sup> Several other biomechanical studies have generally supported the advantages of using a longer screw for S1.<sup>8,28</sup> Therefore, it can be concluded that S1PS placement through the parasagittal approach has several advantages from a biomechanical point of view.

So far as biomechanical advantages are concerned, bicortical fixation of S1PS has also been proved stronger.<sup>10,13</sup> Anatomic constraints, however, should be considered in the case of bicortical fixation. Several authors have recommended that placement of S1PS with a straight-ahead position should be avoided because it carries risks of damage to the iliac vessels, sympathetic chain, and the lumbosacral trunk that are closely applied to the sacrum.<sup>16–19</sup> In the present study, it was confirmed using the measurement of SVD that the interval between the CIV and the anterior sacral cortex was quite short. Therefore, we should be careful not to insert an overlong screw. However, based on the anatomic study by Mirkovic *et al*, it may be safe for a screw to penetrate the anterior sacral cortex within 22 mm of the midline.<sup>16</sup> These authors did not, however, refer to the difference in the anatomic location of the right and left common iliac vessels. Licht *et al* mentioned that the left CIV was at high risk at the S1 level because of the orientation of the

vein across the anterior body of S1 after diverging from the inferior vena cava.<sup>19</sup> In the present study, the shortest distance from the midline to the left CIV (mean MVD; 19.5 mm), was indeed found to be significantly less than that to the right CIV (mean MVD 23.6 mm). This implies that the safe zone on the left side, at least for Japanese patients, is an even narrower range than Mirkovic *et al* suggested. According to the evaluation of LED, the S1PS tip in the midline approach pierced through an anterior sacral cortex laterally further from the midline than in the parasagittal approach. The fact that the mean value of LED (18.9 mm) in the midline approach was remarkably close to the left MVD (19.5 mm) is worthy of note. The present results indicate that there is a risk of injury to the left CIV in case of a bicortical S1PS placement in particular by the midline approach. Four left screws (15.4%) in the patients treated with the midline approach actually made contact with the left CIV, whereas no screw did in the parasagittal approach group. We emphasize that the medially oriented S1PS placement obtained with the parasagittal approach is very useful from the viewpoint of safety as well as mechanical strength.

There are some limitations in this study that deserve mention. First, major one is that this study had a retrospective design, with historical controls. The type of PS, the CT scanner, the surgeon, and the anatomy of the patients were not standardized. However, even under the blind prospective study, the surgeon-related bias does not become negligible because the surgeons would probably handle the PS angle intentionally if they know the purpose of the study in advance. To control the experimental condition and to reduce the bias, *in vitro* study using cadaver may be applicable. Second, the long-term outcomes of the 2 groups regarding instrumentation failure, bone union at the level of fusion, and clinical results were not investigated. Last, when it was difficult to accurately determine the rim of the CIV as described above, we were forced to exclude several cases.

## ■ Conclusion

To our knowledge, the current study is the first report that compares the parasagittal muscle-splitting approach with the conventional midline approach for S1PS placement. Our results demonstrate that the former may be superior to the latter with more medially oriented S1PS placement, which will provide stronger and safer fixation.

## ■ Key Points

- The positions of S1 pedicle screws inserted by a parasagittal approach were compared with those inserted using a midline approach using postoperative CT images along the screw axis.

- The paraspinal approach can lead to more medially oriented S1 pedicle screw placement than the midline approach, which should provide stronger fixation.
- Medially oriented S1 pedicle screw placement can be performed with less risk to the iliac vein, particularly on the left side, even with bicortical fixation.

## References

- Beguristain JL, Martinez-Peric R, Barrios RH, et al. Lumbosacral arthrodesis with Louis technique. *Eur Spine J* 1994;3:169-71.
- Ogilvie JW, Schengel M. Comparison of lumbosacral fixation devices. *Clin Orthop Relat Res* 1986;203:120-5.
- Jackson RP, Hamilton AC. CD screws with oblique canal for improved sacral fixation: a prospective clinical study of the first fifty patients. In: *Seventh Proceeding of the International Congress on Cotrel-Dubousset Instrumentation*. Montpellier, France: Sauramps Medical; 1990:75-86.
- Emami A, Deviren V, Berven S, et al. Outcome and complications of long fusions to the sacrum in adult spine deformity: luque-galveston, combined iliac and sacral screws, and sacral fixation. *Spine* 2002;27:776-86.
- Devlin VJ, Boachie-Adjei O, Bradford DS, et al. Treatment of adult spinal deformity with fusion to the sacrum using CD instrumentation. *J Spinal Disord* 1991;4:1-14.
- Carlson GD, Abitbol JJ, Anderson DR, et al. Screw fixation in the human sacrum: an in vitro study of the biomechanics of fixation. *Spine* 1992; 17(Suppl):S197-203.
- Peretti F, Argenson C, Bourgeon A, et al. Anatomic and experimental basis for the insertion of a screw at the first sacral vertebra. *Surg Radiol Anat* 1991;13:133-7.
- Lehman RA, Kuklo TR, Belmont PJ Jr, et al. Advantage of pedicle screw fixation directed into the apex of the sacral promontory over bicortical fixation. *Spine* 2002;27:806-11.
- Von Stempel A, Trenkmann S, Kronauer I, et al. The stability of bone screws in the so sacrum. *Eur Spine J* 1998;7:313-20.
- Zindrick MR, Wiltse LL, Widell EH, et al. A biomechanical study of intrapedicular screw fixation in the lumbosacral spine. *Clin Orthop Relat Res* 1986;203:99-111.
- Ruland CM, McAfee PC, Warden KE, et al. Triangulation of pedicular instrumentation: a biomechanical analysis. *Spine* 1991;16(6 Suppl):S270-6.
- Smith SA, Abitbol JJ, Carlson GD, et al. The effects of depth of penetration, screw orientation, and bone density on sacral screw fixation. *Spine* 1993;18: 1006-10.
- Zheng YZ, Lu WW, Zhu Q, et al. Variation in bone mineral density of the sacrum in young adults and its significance for sacral fixation. *Spine* 2000; 25:353-7.
- Barber JW, Boden SD, Ganey T, et al. Biomechanical study of lumbar pedicle screws: does convergence affect axial pullout strength? *J Spinal Disord* 1998; 11:215-20.
- Luk KD, Chen L, Lu WW. A stronger bicortical sacral pedicle screw fixation through the S1 endplate. *Spine* 2005;30:525-9.
- Mirkovic S, Abitbol JJ, Strinman J, et al. Anatomic consideration for sacral screw placement. *Spine* 1991;16(6 Suppl):S289-94.
- Esses SI, Botsford DJ, Huller RJ, et al. Surgical anatomy of the sacrum. A guide for rational screw fixation. *Spine* 1991;16(6 Suppl):S283-8.
- Ergur I, Alkali O, Kiray A, et al. Neurovascular risks of sacral screws with bicortical purchase: an anatomical study. *Eur Spine J* 2007;16:1519-23.
- Licht NJ, Rowe DE, Ross LM. Pitfalls of pedicle screw fixation in the sacrum. A cadaver model. *Spine* 1992;17:892-6.
- Wiltse LL, Bateman JG, Hutchison RH, et al. The paraspinal sacrosplintersplitting approach to the lumbar spine. *J Bone Joint Surg* 1968;50:919-26.
- Vialle R, Wicart P, Drain O, et al. The Wiltse paraspinal approach to the lumbar spine revisited. *Clin Orthop Relat Res* 2006;445:175-80.
- Foley KT, Holly LT, Schwender JD. Minimally invasive lumbar fusion. *Spine* 2003;28:26-35.
- Hyun SJ, Lim YB, Kim YS, et al. Postoperative changes in paraspinal muscle volume: comparison between paramedial interfacial and midline approaches for lumbar fusion. *J Korean Med Sci* 2007;22:646-51.
- Datta G, Gnanalingham KK, Peterson D, et al. Back pain and disability after lumbar laminectomy: is there a relationship to muscle retraction? *Neurosurgery* 2004;54:1413-20.
- Weaver EN Jr. Lateral intramuscular planar approach to the lumbar spine and sacrum. *J Neurosurg Spine* 2007;7:270-3.
- Robertson PA, Plank LD. Pedicle screw placement at the sacrum: anatomical characterization and limitations at S1. *J Spinal Disord* 1999;12:227-33.
- Kaptanoglu E, Okutan O, Tekdemir I, et al. Closed posterior superior iliac spine impeding pedicular/porous S-1 screw insertion. *J Neurosurg* 2003;99: 229-34.
- Asher MA, Strippen WE. Anthropometric studies of the human sacrum relating to dorsal transsacral implant. *Clin Orthop Relat Res* 1986;203: 58-62.
- Xu R, Ebraheim NA, Mohamed A, et al. Anatomic considerations for dorsal sacral plate-screw placement. *J Spinal Disord* 1995;8:352-6.
- Krag MH, Beynon BD, Pope MH, et al. Depth of insertion of transpedicular vertebral screws into human vertebrae: effect upon screw-vertebra interface strength. *J Spinal Disord* 1989;1:287-94.

---

# Reinforcement of tendon attachment to bioactive porous titanium by BMP-2-induced ectopic bone formation

---

Kazutaka So,<sup>1</sup> Mitsuru Takemoto,<sup>1</sup> Shunsuke Fujibayashi,<sup>1</sup> Masashi Neo,<sup>1</sup> Tadashi Kokubo,<sup>2</sup> Takashi Nakamura<sup>1</sup>

<sup>1</sup>Department of Orthopaedic Surgery, Graduate School of Medicine, Kyoto University, 54 Shogoin-kawahara-cho, Sakyo-ku 606-8507, Kyoto, Japan

<sup>2</sup>Department of Biomedical Sciences, College of Life and Health Sciences, Chubu University, 1200 Matsumoto-cho, Kasugai 487-8501, Aichi, Japan

Received 21 April 2008; revised 25 July 2009; accepted 26 August 2009

Published online 12 November 2009 in Wiley InterScience (www.interscience.wiley.com). DOI: 10.1002/jbm.a.32640

**Abstract:** Achieving a firm attachment between a tendon and a metal remains a major challenge in orthopedic surgery. In this study, we developed a simple model for evaluating the strength of this attachment using bioactive porous titanium, and confirmed whether bone morphogenic protein-2 (BMP-2) can be a help in achieving a firm attachment by ectopic bone formation. Rectangular plate-shaped implants were soak-loaded with BMP-2 (B+ group) and were implanted within the patellar tendon of a rabbit. Implants without BMP-2 (B- group) were used as controls, and they were harvested at 4 and 8 weeks postoperation for mechanical tests and for histological and histomor-

phometric study. The pull-out failure load of the B+ group was significantly higher than that of the B- group and new bone was more prevalent within the pores and around the implants in the B+ group than in the B- group. The model used in this study was feasible for evaluating the tendon-metal attachment, and a combination of bioactive porous titanium and BMP-2 was found to attach firmly to the tendon. © 2009 Wiley Periodicals, Inc. *J Biomed Mater Res* 93A: 1410–1416, 2010

**Key words:** tendon; titanium; BMP (bone morphogenic protein); mechanical test; drug delivery

---

## INTRODUCTION

In prosthetic surgeries involving malignant bone tumors and comminuted fractures of the proximal humeral bone, firm attachment between the tendon and the metal prosthesis is necessary to enhance joint stability and control of the limb. However, the solution to this challenge has not been realized<sup>1,2</sup> because tendon-tissue is poor in vascularity and healing ability,<sup>3,4</sup> and the prosthesis is poorer still. To solve this problem, a new material and a new method have been proposed in previous papers.<sup>5–9</sup> Some of these studies show that the attachment can be reinforced by interposing bone between the tendon and the metal. For this method to be successful, bone should not only be interposed, but also attach firmly to both the tendon and the metal *in vivo*.

Interposed bone has been mainly supplied by autograft or allograft in the previous studies.<sup>6–9</sup> However, bone grafting does not solve all problems such as donor site morbidity, additional required procedures, and the long time required for the grafted bone to be revascularized. For simplicity and reproducibility in this study, we used bone morphogenic protein-2 (BMP-2) to interpose new bone between the tendon and the metal.

Bioactive-treated titanium has been previously demonstrated to attach directly to the bone<sup>10,11</sup> and to have excellent osteoconductivity and osteoinductivity *in vivo*.<sup>12–14</sup> Bioactive porous titanium was tested here as a promising metal that can firmly attach to the tendon via interposed bone.

This study aimed to confirm whether direct and firm attachment between the tendon and the bioactive porous titanium could be formed via bone with addition of BMP-2. A simple experimental model using rabbit patellar tendon was developed to evaluate the attachment. In the model, histological investigations and mechanical tests were performed to evaluate the osteoinductivity of the implant and the pull-out strength of the tendon/implant complex, respectively.

Correspondence to: K. So; e-mail: so\_kazu@kuhp.kyoto-u.ac.jp